Atom profiles of interfaces with polar-angle-dependent photoemission: Au/GaAs(100)

F. Xu, Yoram Shapira,* D. M. Hill, and J. H. Weaver
Department of Chemical Engineering and Materials Science, University of Minnesota, Minneapolis, Minnesota 55455

(Received 24 November 1986)

We present atom distribution profiles, obtained using nondestructive, polar-angle-dependent x-ray photoemission, of Au/GaAs(100)-$c(8\times2)$ interfaces formed at room temperature. The results confirm substrate disruption, the release of Ga and As atoms into the overlayer, and the presence of significant amounts of Ga and As atoms segregated near the vacuum surface. At high Au coverages, our analysis determines the number of segregated Ga and As atoms, shows that the distribution of these atoms decreases exponentially into the Au film ($1/e$ length of ~3 Å) and diminishes with increasing Au thickness, and finds that the solid solubility in the film is 0.2 ± 0.1 at.% for both Ga and As. The heterogeneous profile indicates that the Au/GaAs reaction at the buried interface is very limited and that intermixing in the overlayer is dictated primarily by solubilities.

INTRODUCTION

The interfacial region which forms when metal overlayers are deposited onto semiconductors can have a complex atom profile and exhibit fascinating physical and chemical properties.[1-17] These properties are related, in part, to the metastability of the boundary layer and its limited spatial extent. The many interesting studies of the last decade have produced a number of systematics, and correlations between structure and properties are becoming increasingly possible. At the same time, most studies of interfaces formed at room temperature have examined the various stages of development of the near-surface region. Less is known about the final state of relatively thick films, particularly quantitative information about the atom distribution normal to the surface. Such information is essential if diffusion, intermixing, reaction, and segregation are to be understood.

In this paper, we report a nondestructive, quantitative determination of the atom profile for Au/GaAs(100) based on polar-angle-dependent x-ray photoemission (XPS). With this technique, it is possible to change the surface sensitivity to the measurements by varying the probe depth $\lambda\sin\theta$, where θ is the angle of emission relative to the surface and λ is the photoelectron mean free path. Angle-dependent XPS has been used previously for binary systems[2] and is complementary to other techniques which seek to develop an understanding of the species distribution of evolving interfaces. For the Au/GaAs system, there is a great deal of information which has come from photoelectron spectroscopy,[3-6] Auger spectroscopy,[7,8,15] low- and reflection-high-energy electron diffraction,[9,10] Kelvin probe,[11] surface photovoltage spectroscopy[7,12] transmission electron microscopy,[13] and transport measurements.[14]

Previous reports of Au overlayers of III-V compound semiconductors have shown that Au induces limited substrate disruption but that a continuous Au overlayer forms, starting from the early stages of deposition, with no well-defined compound formation. Preferential surface segregation of As (Ref. 4) or Ga (Ref. 5) has been reported for studies conducted at room temperature. The purpose of this paper is to determine the distribution of those atoms near the surface, near the buried interface, and far from either boundary, without inducing either physical or chemical changes or being limited to the outermost few atomic layers.

EXPERIMENT

The measurements were done using a Surface Science Instruments (SSI) SSX-100-03 x-ray photoelectron spectrometer and monochromatized Al $K\alpha$ radiation (1486.6 eV).[1] The dual-chamber spectrometer has an operating pressure of $\sim6\times10^{-11}$ Torr. Sputter cleaning of the GaAs(100) sample was done in the measurement chamber, and a cryopump provided rapid return of the system to base pressure. Angle profiles were obtained by rotating the sample around its normal with the photon source and electron analyzer held fixed. X-ray spot diameters ranged from 150 μm to 1 mm. The photoelectrons were energy analyzed with the SSI hemispherical analyzer at pass energies between 25 and 150 eV. For room-temperature core-level line-shape studies of Au deposition onto GaAs, we used the highest resolution (and compared the results to our synchrotron radiation photoemission spectra[18]); for studies of intensity profiles, we used lower resolution to maximize the counting rates. Data acquisition was facilitated by a multichannel detector with 128 parallel lines interfaced to a dedicated HP 9835C computer. Spectra could be collected for angles between grazing emission and normal emission. The analyzer half-angle of acceptance was 15°.

GaAs wafers (silicon doped at $\sim10^{18}$ cm^{-3}) oriented to within 0.5° of the (001) plane were etched in a mixture of H_2SO_4:H_2O_2:H_2O (5:1:1) prior to insertion into the spectrometer. Once under UHV conditions, the wafers were cleaned by Ar^+ sputtering and annealing. The sample temperature was determined using an infrared pyrometer which had been calibrated with a thermocouple (accuracy ±15°C). Repetitive cleaning cycles produced a well-

 ©1987 The American Physical Society

ordered GaAs(001)-$c(8\times2)$ reconstruction, as verified with low-energy electron diffraction (LEED), with no detectable carbon and oxygen. Gold was evaporated from a resistively heated W wire basket at pressures less than 1×10^{-10} Torr. The amount of Au deposited was monitored with an Inficon quartz crystal oscillator. The sample to source distance was ~30 cm, and the typical evaporation rate was 1 Å/min.

RESULTS AND DISCUSSION

In Fig. 1 we show the Ga and As $3d$ core level spectra for the clean GaAs(100) surface [bottom set of energy distribution curves (ECD's)] and for a coverage of 60 Å of Au at polar angles of 90°, 50°, and 10° at room temperature. The results for the clean GaAs(100) surface were identical for all the emission angles.[19] Binding energies are referenced to the Ga or As $3d$ position for the clean surface; the EDC's have been normalized to emphasize line-shape changes. For Ga, they show that the deposition of 60 Å of Au induces a chemical shift of approximately -0.4 eV. The corresponding shift for As is effectively zero, in agreement with higher-resolution synchrotron radiation results.[18] The spectra for the clean surface were decomposed into their $3d_{5/2}$ and $3d_{3/2}$ spin-orbit components, as shown by dashed lines. For Ga, the spin-orbit splitting was held to be 0.44 eV, the branching ratio was 1.5, the full width at half maximum (FWHM) for each component was 0.91 eV, and the line shape had 83% Gaussian and 17% Lorentzian character. The corresponding parameters for As were 0.70, 1.5, and 0.91 eV. The deposition of 60 Å of Au resulted in a line-shape narrowing for both Ga and As, with FWHM reductions for Ga to 0.78 eV at 90°, 0.75 eV at 50°, and 0.65 eV at 10° (to 0.82 eV at 90°, 0.81 eV at 50°, and 0.71 eV at 10° for As). Similar line-shape changes were observed at other coverages (not shown). The Au $4f_{7/2}$ emission line shape did not change with coverage. These results support the conclusions of others that Ga and As atoms dissociated from the substrate are dissolved in the growing Au overlayer. At the same time, the persistence of the Ga and As signals to very high coverages also confirms surface segregation of both species. Indeed, recent surface-sensitive synchrotron radiation photoemission results by Grioni *et al.*[18] showed that the emission of Ga had a plateau and the emission from As first diminished, then increased and remained almost constant as segregation occurred.

The results of our polar-angle dependent XPS studies make it possible to be quantitative in describing the atomic profile of the Au overlayer. In Fig. 2 we show representative intensity profiles for low Au coverage (10 and 20 Å) and in Fig. 3 results for higher coverage (80 and 100 Å). In both figures, the vertical axis corresponds to the Ga or As intensity divided by the total As $3d$, Ga $3d$, and Au $4f_{7/2}$ core level emission, with corrections for background subtraction, data acquisition time, and photoionization cross sections. The cross sections were determined by assuming that the atomic densities of Ga and

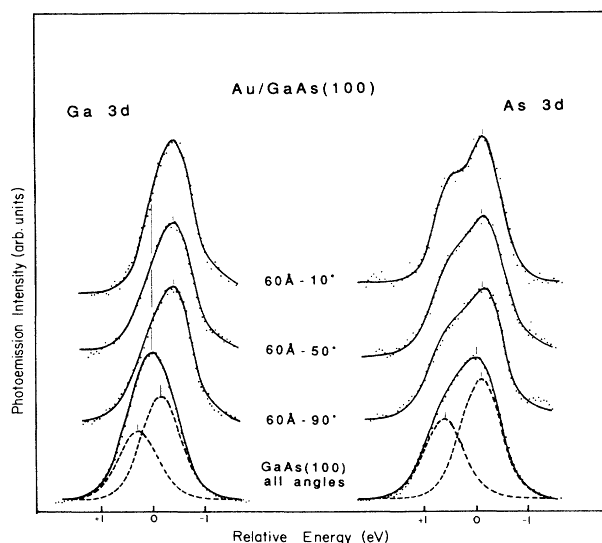

FIG. 1. X-ray photoemission core level spectra for the clean GaAs(100)-8×2 surface, showing the decomposition of the Ga and As $3d$ levels into $d_{3/2}$ and $d_{5/2}$ components (dashed lines). The deposition of 60 Å of Au onto the surface results in a chemical shift for Ga but essentially no shift for As. Spectra taken as a function of angle show that the surface-sensitive results (emission angle of 10° from the horizon) show slightly sharper line shapes. The spectra have been scaled for visual clarity.

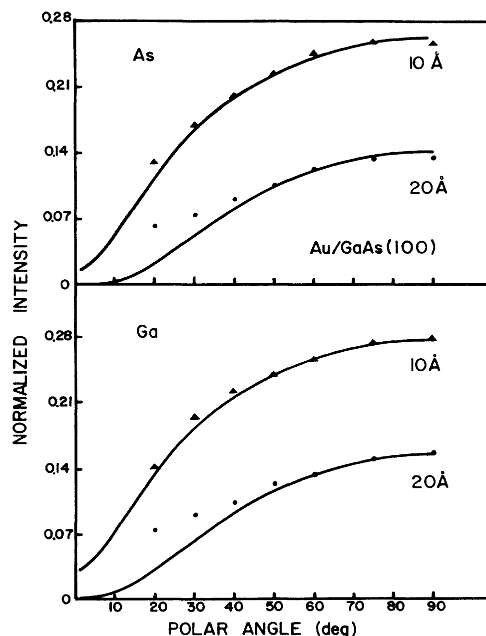

FIG. 2. Normalized total integrated intensities for the Ga and As $3d$ emission as a function of emission angle for low coverage for comparison to Eqs. (7) and (8) of the text. For nominal overlayer thicknesses of 10 and 20 Å, the entire intermixed region is being probed, except at the most grazing of emission angles, and the results show a diminishing Ga and As content of the growing Au film relative to the substrate. The solid lines are fits to the data based on the model profiles of Figs. 4 and 5.

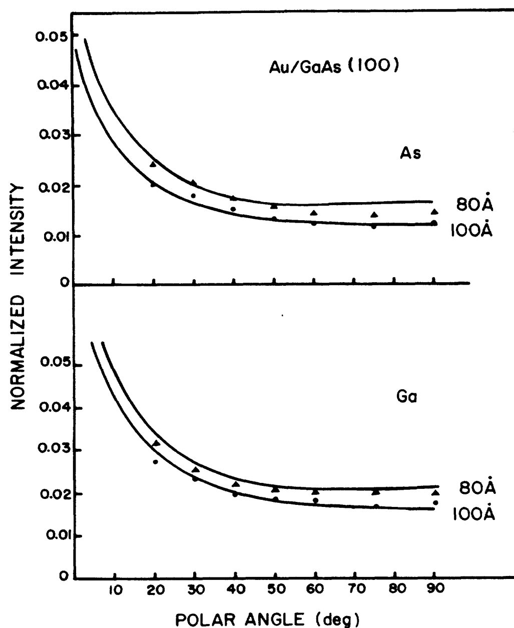

FIG. 3. Normalized total integrated intensities analogous to those of Fig. 2 for thick Au overlayers. As shown, the Ga and As emission increases for grazing emission, indicating that the Ga and As content of the surface region is greater than that of the bulk.

As in the probed region for the initial clean GaAs(100) surface were the same. Thus, $\sigma_{As}/\sigma_{Ga}=I_{As}(\theta)/I_{Ga}(\theta)=1.32\pm0.05$, averaged over different angles. Under the same experimental conditions, we compared the integrated intensity of the Au $4f_{7/2}$ core level at high Au coverage (nominal thickness, a, of 150 Å) to the Ga $3d$ emission for the clean surface. Taking into account the different atomic densities of bulk Au and Ga in GaAs, we determined the cross-section ratio $\sigma_{Au}/\sigma_{Ga}=[I_{Au}(a=150\text{ Å},\theta)/I_{Ga}(a=0\text{ Å},\theta)](\rho^0_{Ga}/\rho^0_{Au})=3.6\pm0.1$. For the results of Fig. 2 at low coverage, there is a substantial contribution from the substrate, except at the lowest angles, and these profiles sample the intermixed region near the disrupted substrate ($\lambda\sin\theta$ ranges from ~17 Å at 90° to ~3 Å at 10°). The results for higher coverage in Fig. 3 detect the Ga and As profiles near the surface for the well-developed Au film.

From our angular-dependent intensity results, the Ga and As attenuation curves,[18] the sputter depth profiling,[3] and other studies of Au/GaAs, a qualitative picture of the phenomena of room-temperature Au deposition onto GaAs can be drawn. As Au atoms are deposited, they disrupt surface Ga—As bonds and create an intermixed layer of Au with dissociated Ga and As. No distinct compound formation is observed at room temperature. Instead, the dissociated semiconductor atoms form a supersaturated solution. As the film grows, some of the semiconductor atoms can be expelled to the surface such that their concentration in the interior of the film more closely approximates the solubility of the bulk film. This represents a lowering of the free energy of the film in cases where solubilities are low and there is little tendency for compound formation. The result can be that the concentration of Ga and As at the free surface increases. The present results, and those for other similar systems, indicate the existence of some onset of the surface segregation process. For Au/GaAs(110), the synchrotron radiation photoemission attenuation curves[18] taken with high surface sensitivity show that the As emission initially decreases but then increases again and holds steady over a wide range of coverages. For Ga, the amount of segregation is lower, but the emission again remains almost constant for coverages exceeding ~20 ML. Once these plateau regions have been reached, the atom distributions near the surface assume well defined and characteristic profiles. The addition of metal atoms from the vapor phase results in the growth of the metal layer and the continued segregation of the semiconductor atoms. Burial of segregated atoms must be related to solubilities.

Angular-dependent XPS intensity measurements make it possible to test this intuitive picture of the evolving interface in a nondestructive way. If the medium is continuous, the photoemission intensity $I_A(\theta)$ of element A measured at an angle θ with respect to the surface can be written

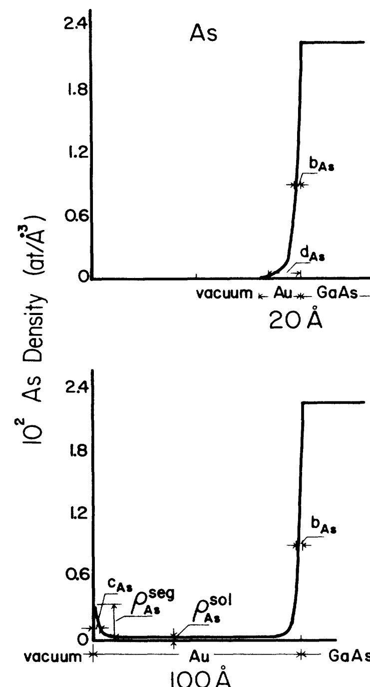

FIG. 4. Model profile showing the exponential decay of the As concentration away from the substrate for a nominal Au coverage of 20 Å (top) with b_{As} defined as the $1/e$ length. When the coverage exceeds the critical value at which surface enrichment relative to the near-surface region sets in, a second exponential function is introduced. A constant value corresponding to the concentration of As in solution is also added (bottom). Modeling is least reliable when the two exponential functions overlap, and this corresponds to the poorly understood onset of surface enrichment.

$$I_A(\theta)=I_0(\theta)\sigma_A S\int_0^\infty \rho_A(z)e^{-z/\lambda\sin\theta}dz\ . \tag{1}$$

σ_A denotes the photoionization cross section, $\rho_A(z)$ describes the density distribution of element A, S is the spot size of the incident x-ray beam, and $I_0(\theta)$ is the intensity of a pure material having unity cross section and unity atomic density.

It should prehaps be reiterated that for the purposes of our mathematical modeling "segregation region" refers to the region in which the semiconductor atom distribution is described by an exponential function which decays away from the free surface into the overlayer. Physically, we know that there are semiconductor atoms on the overlayer surface, even at low coverage, but the concentration of these semiconductor atoms appears to increase as the buried interface is approached. Their presence can therefore be treated mathematically by an exponential function that decays from the buried interface. At high coverage, however, it is impossible to describe the profile of these segregated atoms by a single distribution function. The onset of surface segregation is then defined as the coverage at which the second distribution function is needed and there is clear evidence for the two functional forms.

By keeping in mind the physical picture of the diffusion and segregation described above, we can model the As distribution as shown in Fig. 4. For the simplest model, we assume that the As profiles into Au from either the substrate or the vacuum will be exponential with $1/e$ lengths $b_{\rm As}$ and $c_{\rm As}$, respectively. Hence, the distribution functions at high and low coverage are

$$\rho_{\rm As}^{\rm hi}(z)=\begin{cases}\rho_{\rm As}^{\rm seg}\exp(-z/c_{\rm As})+\rho_{\rm As}^{\rm sol}+\rho_{\rm As}^{0}\exp[(z-a)/b_{\rm As}] & \text{for } z<a\ ,\\ \rho_{\rm As}^{0}\ \text{for } z\geq a\ , \end{cases} \tag{2a}$$

$$\rho_{\rm As}^{\rm lo}(z)=\begin{cases}\rho_{\rm As}^{\rm sol}\ \ \text{for } z<(a-d_{\rm As})\ ,\\ \rho_{\rm As}^{0}\exp[(z-a)/b_{\rm As}]\ \ \text{for } (a-d_{\rm As})<z<a\ ,\\ \rho_{\rm As}^{0}\ \ \text{for } z\geq a\ .\end{cases} \tag{2b}$$

With $\rho_{\rm As}^{\rm seg}=\rho_{\rm As}^{\rm seg}(a)$, we indicate the (overlayer-thickness-dependent) density of segregated As on the free surface; $c_{\rm As}$ is the characteristic decay width of the surface segregation region; $\rho_{\rm As}^{\rm sol}$ is the atomic density of As dissolved in Au and is constant; $\rho_{\rm As}^{0}$ is the atomic density of As in GaAs; and $d_{\rm As}$ denotes the coverage at which the As concentration near the free surface is close to its bulk solubility in Au. z is the distance measured from the vacuum surface.

When intermixing is complete, the total quantity of released As should remain constant, i.e.,

$$S\int_0^{a_1}\rho_{\rm As}^{\rm hi}(z)dz=S\int_0^{a_2}\rho_{\rm As}^{\rm lo}(z)dz=A=\text{const}\ , \tag{3}$$

where a_1 is greater than (a_2 is less than) the coverage at which segregation begins. This relation correlates the two distribution functions at high and low coverages. By using Eq. (2), we obtain

$$\begin{aligned}I_{\rm As}^{\rm hi}&=\sigma_{\rm As}I_{\rm As}^{0}(\theta)=\sigma_{\rm As}I_0(\theta)S\int_0^\infty\rho_{\rm As}^{\rm hi}(z)e^{-z/\lambda\sin\theta}dz\\&=\sigma_{\rm As}I_0(\theta)S(\lambda\sin\theta)\{[\rho_{\rm As}^{\rm seg}c_{\rm As}/(\lambda\sin\theta+c_{\rm As})](1-e^{-a[(1/c_{\rm As})+(1/\lambda\sin\theta)]})\\&\quad+\rho_{\rm As}^{\rm sol}(1-e^{-a/\lambda\sin\theta})+[(\rho_{\rm As}^{0}b_{\rm As})/(\lambda\sin\theta-b_{\rm As})](e^{-a/\lambda\sin\theta}-e^{-a/b_{\rm As}})\\&\quad+\rho_{\rm As}^{0}e^{-a/\lambda\sin\theta}\}\end{aligned} \tag{4a}$$

and

$$\begin{aligned}I_{\rm As}^{\rm lo}(\theta)&=\sigma_{\rm As}I_{\rm As}^{0}(\theta)=\sigma_{\rm As}I_0(\theta)S\int_0^\infty\rho_{\rm As}^{\rm lo}(z)e^{-z/\lambda\sin\theta}dz\\&=\sigma_{\rm As}^{0}I_0(\theta)S(\lambda\sin\theta)\rho_{\rm As}^{0}\{[b_{\rm As}/(\lambda\sin\theta-b_{\rm As})](e^{-a/\lambda\sin\theta}-e^{-a/b_{\rm As}})+e^{-a/\lambda\sin\theta}\}\ .\end{aligned} \tag{4b}$$

Further, for high coverage we have $b_{\rm As}(a)=b_{\rm As}^{0}=\text{const}$ so that

$$\int_0^a[\rho_{\rm As}^{\rm seg}\exp(-z/c_{\rm As})+\rho_{\rm As}^{\rm sol}]S\,dz=A-\rho_{\rm As}^{0}b_{\rm As}^{0}[1-\exp(-a/b_{\rm As}^{0})]S\ .$$

When $a\gg b_{\rm As}^{0}$ and $a\gg c_{\rm As}$, this reduces to $\rho_{\rm As}^{\rm seg}c_{\rm As}+\rho_{\rm As}^{\rm sol}a=A/S-b_{\rm As}^{0}\rho_{\rm As}^{0}$ and

$$\rho_{\rm As}^{\rm seg}=(A/S-\rho_{\rm As}^{0}b_{\rm As}^{0}-\rho_{\rm As}^{\rm sol}a)/c_{\rm As}\ . \tag{5}$$

For Au/GaAs(100), the distribution of Ga is quite similar to As, as shown in Figs. 2 and 3, because there is no apparent formation of a Au-Ga compound at room temperature. Hence, very similar fitting can be done for the Ga distribution using the distribution function of Fig. 5.

For the Au intensities, we use the bulk value for the density, $\rho_{\rm Au}^{0}=0.059$ atoms/Å^3, so that

$$\begin{aligned}I_{\rm Au}(\theta)&=\sigma_{\rm Au}I_{\rm Au}^{0}(\theta)\\&=\sigma_{\rm Au}I_{\rm Au}^{0}(\theta)S\int_0^\infty\rho_{\rm Au}e^{-z/\lambda\sin\theta}dz\\&=\sigma_{\rm Au}I_0(\theta)S(\lambda\sin\theta)\rho_{\rm Au}^{0}(1-e^{-a/\lambda\sin\theta})\ .\end{aligned} \tag{6}$$

Finally, the normalized intensities for the Ga and As emission measured at any detection angle can be predicted from

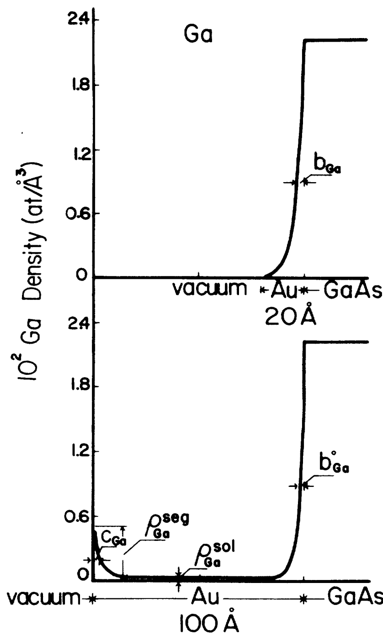

FIG. 5. Ga model profiles analogous to those for As in Fig. 4.

$$D_{\rm Ga}(\theta)=[I^0_{\rm Ga}(\theta)]/[I^0_{\rm Ga}(\theta)+I^0_{\rm As}(\theta)+I^0_{\rm Au}(\theta)]\ , \qquad (7)$$

$$D_{\rm As}(\theta)=[I^0_{\rm As}(\theta)]/[I^0_{\rm Ga}(\theta)+I^0_{\rm As}(\theta)+I^0_{\rm Au}(\theta)]\ . \qquad (8)$$

These expressions can be compared directly to the experimental results. The fitting results for Ga and As based on this model are shown as solid curves in Fig. 2 for Au coverages of 10 and 20 Å and in Fig. 3 for coverages of 80 and 100 Å. The photoelectron mean free path was 17 Å.[20]

The fittings are done in such a way that a satisfactory value of b is sought for low coverages so that the total quantity of released Ga or As can be calculated. By using Eqs. 2(a) and 3, we can obtain the rest of the fitting parameters for high coverage. Our results indicate that the characteristic decay distances are $b_{\rm As}=3$ Å and $b_{\rm Ga}=4$ Å when the Au coverage is 10 Å. For 80- and 100-Å coverages, $c_{\rm As}=c_{\rm Ga}=3$ Å and $\rho^{\rm sol}_{\rm Ga}=\rho^{\rm sol}_{\rm As}=1.3\times10^{-4}$ atoms/Å^3. The latter corresponds to a solid solubility of 0.2 ± 0.1 at. %. The total amount of Ga and As disrupted from the substrate corresponds to 0.08 and 0.06 atoms/Å^2 or the equivalent of about 1.3 and 1 ML of GaAs(100), respectively. The difference between the two total quantities can be understood in terms of the excess Ga content of the reconstructed GaAs(100)-$c(8\times2)$ surface. This suggests that the state of the surface before metal deposition influences the amount of surface segregation in those cases where solubilities dictate atomic profiles. The prediction that the extent of disruption is small is consistent with the observation of Andersson and Svensson that Au can be grown epitaxially on GaAs(100).[10]

From the literature,[21,22] we find that the solubility of Ga in α-phase Au reaches a maximum of 12 at. % at 688.5 K. Extrapolating to room temperature, we expect a solubility of ~0.8 at. %, in good agreement with our interface-determined value. On the other hand, the equilibrium As solubility is very low in Au at elevated temperature and the value extrapolated to room temperature is negligible. As reported in other cases, however, the real solubility at low temperature can be much higher than the extrapolation value.[23]

For the low coverage fittings in Fig. 2, we used solution onsets $d_{\rm As}$ of 15 Å and $d_{\rm Ga}$ of 21 Å which were estimated in such a way that $\rho^0_{\rm As}\exp(-d_{\rm As}/b_{\rm As})=\rho^{\rm sol}_{\rm As}$ and $\rho^0_{\rm Ga}\exp(-d_{\rm Ga}/b_{\rm Ga})=\rho^{\rm sol}_{\rm Ga}$ by assuming $b_{\rm As}=3$ Å and $b_{\rm Ga}=4$ Å, respectively. The discrepancy at grazing angles may be due to the cutoff of the exponential tail; this could be treated mathematically as a reflection at the surface, but such a calculation is beyond our simple model and can be obscured by experimental errors and heterogeneities along the surface.

This simple model assumes that the Au/GaAs interface is abrupt and that there is no metal in-diffusion. In fact, surface disruption does occur and the distance between the vacuum and the buried interface should be greater than the nominal coverage value a. However, the deposited Au leads to relatively limited substrate disruption, as the small amounts of released Ga and As indicate, and for Au coverages larger than the amount of disrupted surface this assumption does not restrict severely the use of the model. Unfortunately, we cannot fit our experimental results in the intermediate coverage range because of inadequate information about the onset of surface segregation. We estimate that this segregation begins at ~20 Å. By ~60 Å, $\rho^{\rm seg}(a)$ starts to decrease as atoms dissolve in the growing Au film.

Support for these estimates comes from the surface-sensitive synchrotron radiation results which show that the attenuation curve of total As intensity initially decreases then increases and, finally, decreases again with coverage.[3,18] Shapira *et al.*[12] recently reported qualitatively similar results of anion and cation distributions in the growing Au overlayer for the system Au/InP(110). Their Auger sputtering profiles showed that enrichment of the surface relative to the bulk (our definition of surface segregation) was not apparent for Au thicknesses below about 30 Å, in analogy with our findings for Au/GaAs (they also discussed profile broadening due to the sputtering process). Further, the number of surface-segregated atoms was observed to decrease very slowly with coverage due to their low solubility in Au. Additional support comes from the results of Kobayashi *et al.*[16] for Au/GaAs which showed the persistence of As at high coverage due to surface segregation. Rutherford backscattering measurements were in agreement with this interpretation. These authors also remarked that there was no surface As signal for Au coverages of less than 25 ML, consistent with our picture. The relative absence of Ga on their surface can perhaps best be understood in terms of the different initial surface [(100) versus (110)], as discussed.

In conclusion, our polar-angle-dependent x-ray photoemission results show the effects of Au deposition onto GaAs(100) at room temperature. Although we find no evidence for compound formation, we observe disruption

of the surface with dissociated Ga and As atoms dissolved in the Au matrix and segregated to the surface. Characterizing the atom profile near the vacuum surface, we find that the concentration of both Ga and As decreases exponentially with distance into the Au film and we determined the characteristic decay lengths. Further, we determined the solubility of Ga and As in Au far from either the buried interface or the surface, finding 0.2 ± 0.1 at. %.

ACKNOWLEDGMENTS

This work was supported by the Office of Naval Research under Grants No. ONR-N00014-87-K-0029 and No. N00014-86-K-0427 and the Minnesota Microelectronic and Information Sciences Center. Y.S. is grateful for support of the Belfer Center for Energy Research, Israel and Kernforschungsanlage Jülich, Germany.

---

*Permanent address: Faculty of Engineering, Tel Aviv University, Ramat Aviv 69978, Israel.

[1]L. J. Brillson, Surf. Sci. Rep. **2**, 123 (1982), and extensive references therein. J. H. Weaver, Phys. Today **39**(1), 24 (1986); a photo of the XPS experimental system used for these studies is shown on the cover of that issue.

[2]J. M. Hill, D. C. Royce, C. S. Fadley, L. F. Wagner, and F. J. Grunthaner, Chem. Phys. Lett. **44**, 225 (1976); H. Iwasaki, R. Nishitani, and S. Nakamura, Jpn. J. Appl. Phys. **17**, 1519 (1978); T. D. Bussing and P. H. Holloway, J. Vac. Sci. Technol. A **3**, 1973 (1985).

[3]P. W. Chye, I. Lindau, P. Pianetta, C. M. Garner, C. Y. Su, and W. E. Spicer, Phys. Rev. B **10**, 5545 (1978); T. Kendelewicz, W. G. Petro, I. Lindau, and W. E. Spicer, J. Vac. Sci. Technol. B **2**, 453 (1984); W. G. Petro, T. Kendelewicz, I. Lindau, and W. E. Spicer, Phys. Rev. B **34**, 7089 (1986).

[4]W. G. Petro, I. A. Babalola, T. Kendelewicz, I. Lindau, and W. E. Spicer, J. Vac. Sci. Technol. A **1**, 1181 (1983); T. Narusawa, N. Watanabe, K. L. I. Kobayashi, and H. Nakashima, *ibid.* **2**, 538 (1984).

[5]A. Hiraki, S. Kim, W. Kammura, and M. Iwami, Surf. Sci. **86**, 706 (1979).

[6]L. J. Brillson, P. S. Bauer, R. Z. Bachrach, and G. Hansson, Phys. Rev. B **23**, 6204 (1981).

[7]W. Mönch, Thin Solid Films **104**, 285 (1983).

[8]Y. Shapira and L. J. Brillson, J. Vac. Sci. Technol. B **1**, 618 (1983); Y. Shapira, L. J. Brillson, A. D. Katnani, and G. Margaritondo, Phys. Rev. B **30**, 4586 (1984).

[9]A. Kahn, C. R. Bonapace, C. B. Duke, and A. Paton, J. Vac. Sci. Technol. B **1**, 613 (1983).

[10]T. G. Andersson and S. P. Svensson, Surf. Sci. Lett. **110**, L583 (1981); T. G. Andersson, J. Kanski, G. LeLay, and S. P. Svensson, Surf. Sci. **168**, 301 (1986).

[11]L. Lassabatere, J. M. Palau, E. Vienjot-Testermale, A. Ismail, C. Raisin, J. Bonnet, and L. Soonckindt, J. Vac. Sci. Technol. B **1**, 549 (1983).

[12]Y. Shapira, L. J. Brillson, and A. Heller, Appl. Phys. Lett. **43**, 174 (1983).

[13]T. Yoshiie and C. L. Bauer, J. Vac. Sci. Technol. A **1**, 554 (1983); T. Yoshiie, C. L. Bauer, and A. G. Milnes, Thin Solid Films **11**, 149 (1984); S. Leung, D. L. Chung, and A. G. Milnes, *ibid.* **104**, 109 (1983).

[14]R. H. Williams, R. R. Varma, and A. McKinley, J. Phys. C **10**, 4545 (1977).

[15]J. R. Lince, C. T. Tsai, and R. S. Williams, J. Mater. Res. **1**, 537 (1986).

[16]N. Watanabe, K. L. I. Kobayashi, T. Narusawa, and H. Nakashima, J. Appl. Phys. **58**, 3766 (1985); K. L. I. Kobayashi, N. Watanabe, T. Narusawa, and H. Nakashima, *ibid.* **58**, 3758 (1985).

[17]S. A. Chambers, D. M. Hill, F. Xu, and J. H. Weaver, Phys. Rev. B **35**, 634 (1987).

[18]See M. Grioni, J. J. Joyce, and J. H. Weaver, J. Vac. Sci. Technol. A **4**, 965 (1986), for synchrotron radiation photoemission results for Au/GaAs(110). See also Ref. 3.

[19]We did not detect changes in line shape at grazing emission due to surface-shifted substrate atoms for GaAs(100).

[20]W. M. Riggs and M. J. Parker, in *Methods in Surface Analysis*, edited by A. W. Czanderna (Elsevier, Amsterdam, 1975).

[21]C. J. Cooke and W. Hume-Rothery, J. Less-Common Metals **10**, 42 (1966).

[22]M. Hansen, *Constitution of Binary Alloys* (McGraw-Hill, New York, 1958); W. G. Moffatt, *Binary Phase Diagrams Handbook* (General Electric Co., Schenectady, 1977).

[23]S. E. R. Hiscocks and W. Hume-Rothery, Proc. R. Soc. London, Ser. A **282**, 318 (1964), reported the solubility of In in Au to be 12.7 at. % at 963 K, giving an extrapolated value of 0.49 at. % at 373 K. Experimental values as high as 9 at. % have been observed.